

# Modeling and Optimal Design of Piezoelectric Cantilever Microactuators

Don L. DeVoe and Albert P. Pisano

**Abstract**—A novel model is described for predicting the static behavior of a piezoelectric cantilever actuator with an arbitrary configuration of elastic and piezoelectric layers. The model is compared to deflection measurements obtained from 500- $\mu\text{m}$ -long ZnO cantilever actuators fabricated by surface micromachining. Modeled and experimental results demonstrate the utility of the model for optimizing device design. A discussion of design considerations and optimization of device performance is presented. [233]

**Index Terms**—Actuator, bimorph, cantilever, model, piezoelectric, ZnO.

## I. INTRODUCTION

THE STATIC analysis of piezoelectric cantilever actuators is typically performed using an approach employed by Timoshenko for calculating the deflection of a thermal bimorph [1]. In Timoshenko's analysis, the principal of strain compatibility is employed between two cantilever beams joined along the bending axis. The deflection of the two-layer structure due to forces generated by one or both of the layers is then determined from static equilibrium. For the case of a piezoelectric heterogeneous bimorph, the structure of interest consists of a piezoelectric layer bonded to a purely elastic layer. The purpose of the elastic layer is, in essence, to offset the neutral axis of the two-layer system so that a lateral strain produced by piezoelectric effect is translated into an applied moment on the bimorph. Such structures are commonly used in macroscale applications such as active structural damping and precision positioning systems. For these macrodevices, the two-layer Timoshenko model (bimorph model) is sufficient for determining the quasi-static behavior of the system since any additional (e.g., bonding) layers are relatively thin and can be ignored. However, for micromachined devices, the bimorph assumption is quite often invalid since such devices may consist of additional layers with thicknesses on the same order as the piezoelectric film itself.

The motivation of this work is to develop a model for multiple-layer cantilever devices, or *multimorphs*, which is applicable to thin-film devices. This model can then be used to investigate optimal film thicknesses for these devices. To avoid confusion, the term *multimorph* is used here to

describe the full class of piezoelectric cantilever devices with an arbitrary configuration of piezoelectric and elastic layers, including bimorphs. Similar devices have been analyzed by several authors. Chu [2] presents a model based directly on Timoshenko's approach, which predicts the static deflection of a micromachined thermal bimorph, the results of which are also applicable to piezoelectric actuators. Smits provides an elegant derivation of the static [3] and dynamic [4] behavior of bimorph structures from basic thermodynamic principles although the analysis does not extend directly to more complex multimorph structures. In this work, a multimorph model is derived, and theoretical results from the model are compared to experimental measurements from 500- $\mu\text{m}$ -long surface-micromachined multimorphs with varying ZnO thicknesses. Based on experimental results, the utility of the model as a design tool for specifying the optimal piezoelectric film thickness is demonstrated.

## II. PIEZOELECTRIC MULTIMORPH MODEL

A model describing the deflection of a piezoelectric multimorph structure can be derived by appealing to the basic mechanics principles of: 1) static equilibrium and 2) strain compatibility between successive layers in the device. In this sense, the approach is similar to Timoshenko's well-known derivation for thermal bimorph deflections, but extended to be applicable to an  $m$ -layer multimorph rather than a simple bimorph.

The basic geometry of an  $m$ -layer multimorph is shown in Fig. 1. In this figure, the individual layers may be either piezoelectric or purely elastic. In the formulation of this model, it is assumed that shear effects are negligible, residual stress-induced curvature may be ignored, beam thickness is much less than the piezoelectric-induced curvature, second-order effects such as electrostriction are negligible, and  $xz$ -plane strain and  $xy$ -plane stress are enforced. Under the assumptions of  $xy$ -plane stress and  $xz$ -plane strain, which are reasonable for a wide flat beam, it can be shown that (1) and (2) hold. The effective modulus for the  $i$ th layer ( $E_i$ ) and transverse-piezoelectric-coupling coefficient ( $d_{31}$ ) given by these equations assume an isotropic Poisson's ratio ( $\nu_i$ ) and are implicitly employed in the derivation of this model

$$E_i \rightarrow E_i / (1 - \nu_i^2) \quad (1)$$

$$d_{31} \rightarrow d_{31} (1 + \nu_i). \quad (2)$$

With the above assumptions outlined, the derivation proceeds as follows. First, it is noted that both axial forces and moments at any cross section of the  $m$ -layer beam shown in

Manuscript received September 17, 1996; revised May 20, 1997. Subject Editor, R. O. Warrington.

D. L. DeVoe is with the Department of Mechanical Engineering, University of Maryland at College Park, College Park, MD 20742 USA.

A. P. Pisano is with the Berkeley Sensor and Actuator Center and Department of Mechanical Engineering, University of California at Berkeley, Berkeley, CA 94720 USA.

Publisher Item Identifier S 1057-7157(97)06329-4.

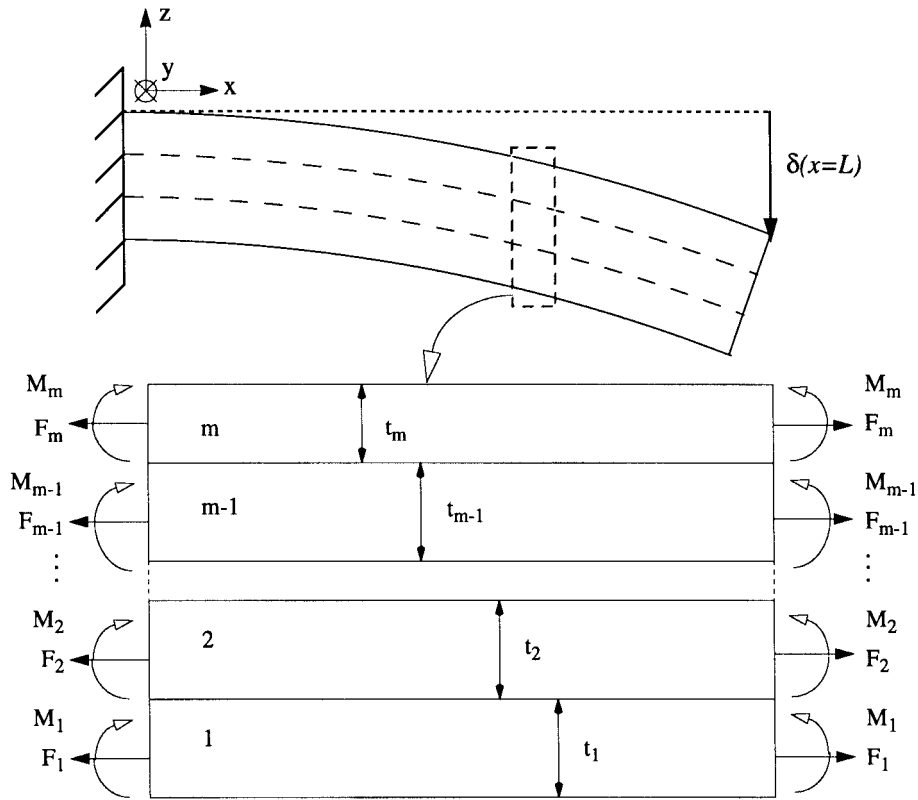


Fig. 1. Generic multimorph geometry and cross section.

Fig. 1 must sum to zero at equilibrium, as expressed in (3) and (4)

$$\sum_{i=1}^m F_i = 0 \quad (3)$$

$$\sum_{i=1}^m M_i = F_1 \left( \frac{t_1}{2} \right) + F_2 \left( t_1 + \frac{t_2}{2} \right) + \dots + F_m \left( \sum_{i=1}^{m-1} t_i + \frac{t_m}{2} \right). \quad (4)$$

The individual moments are related to the curvature,  $1/r$ , by (5), where  $E_i I_i$  is defined as the flexural rigidity of the  $i$ th layer in the beam relative to the beam's neutral axis. Note that the radius of curvature  $r$  is approximately equal for each layer in the structure since it was assumed that the beam thickness is much less than the overall beam curvature

$$\frac{1}{r} = \frac{M_i}{E_i I_i} \quad \text{or} \quad M_i = \frac{E_i I_i}{r}. \quad (5)$$

Equations (4) and (5) may be combined to express the beam equilibrium in terms of axial forces and curvature only as shown in

$$\frac{1}{r} \sum_{i=1}^m E_i I_i = F_1 \left( \frac{t_1}{2} \right) + F_2 \left( t_1 + \frac{t_2}{2} \right) + \dots + F_m \left( \sum_{i=1}^{m-1} t_i + \frac{t_m}{2} \right). \quad (6)$$

Equation (6) can be solved for the curvature as a function of the unknown  $F_i$ 's and rewritten in matrix form as

$$\frac{1}{r} = \frac{1}{\sum_{i=1}^m E_i I_i} \left[ \left( \frac{t_1}{2} \right) \left( t_1 + \frac{t_2}{2} \right) \dots \left( \sum_{i=1}^{m-1} t_i + \frac{t_m}{2} \right) \right] \cdot \begin{bmatrix} F_1 \\ F_2 \\ \dots \\ F_m \end{bmatrix} \equiv \mathbf{D}\mathbf{F}. \quad (7)$$

In (7),  $\mathbf{F}$  is the column vector of axial forces, while  $\mathbf{D}$  is the premultiplication row vector operating on  $\mathbf{F}$ , which is a function of beam geometry and flexural rigidity.

An additional set of  $m - 1$  equations constraining  $1/r$  and the  $m \times 1$  axial force vector  $\mathbf{F}$  follow from the requirement of strain compatibility at the  $m - 1$  interfaces between each set of adjacent layers. The total strain at the surface of each layer is given by superposition of the strain due to the piezoelectric effect, axial force, and bending. This surface strain is given by (8), noting that the sign of the strain due to bending will depend on whether the top or bottom face of the layer is under observation

$$\varepsilon_i = \varepsilon_{\text{piezo}} + \varepsilon_{\text{axial}} + \varepsilon_{\text{bend}} = d_{31} \mathbf{E}_i + \frac{F_i}{A_i E_i} \pm \frac{t_i}{2r}. \quad (8)$$

In (8), the linear constitutive equations for a piezoelectric material [5] have been employed to express  $\varepsilon_{\text{piezo}}$  in terms of the transverse-piezoelectric-coupling coefficient  $d_{31}$  and the electric field applied across the thickness of the layer  $\mathbf{E}_i$ .

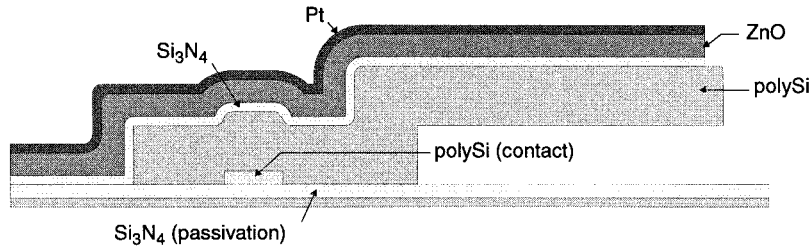


Fig. 2. Experimental four-layer multimorph structure.

Equating the strain at the interface between the  $i$ th and  $(i+1)$ th layers results in

$$d_{31}\mathbf{E}_i + \frac{F_i}{A_i E_i} - \frac{t_i}{2r} = d_{31}\mathbf{E}_{i+1} + \frac{F_{i+1}}{A_{i+1} E_{i+1}} + \frac{t_{i+1}}{2r}. \quad (9)$$

Collecting similar terms in (9) and placing the result into matrix form yields the expression shown at the bottom of the page.

Note that in addition to strain compatibility, this matrix equation also incorporates the expression for axial force equilibrium, given by (3), in the  $m$ th row. Note also that the electric field in the  $i$ th layer  $\mathbf{E}_i$  is nonzero only for piezoelectric layers. Strictly, of course, this is not true, but a field in a purely dielectric material has no effect on multimorph deflection, provided electrostriction effects are negligible. This expression can be rewritten by defining matrices  $\mathbf{A}$ ,  $\mathbf{B}$ , and  $\mathbf{C}$  such that

$$\mathbf{A}\mathbf{F} - \frac{1}{2r}\mathbf{B} - d_{31}\mathbf{C} = \mathbf{0}. \quad (10)$$

Combining (7) and (10) and solving for the curvature yields

$$\frac{1}{r} = \frac{2d_{31}\mathbf{D}\mathbf{A}^{-1}\mathbf{C}}{2 - \mathbf{D}\mathbf{A}^{-1}\mathbf{B}} \quad (11)$$

where  $\mathbf{A}$  is always nonsingular for physically valid choices of  $A_i$  and  $E_i$ .

From the equation for deflection of a simple cantilever beam with constant curvature, the deflection of the multimorph is found directly from the curvature given by (11) as

$$\delta(x) = \frac{x^2}{2r} = x^2 \left[ \frac{d_{31}\mathbf{D}\mathbf{A}^{-1}\mathbf{C}}{2 - \mathbf{D}\mathbf{A}^{-1}\mathbf{B}} \right]. \quad (12)$$

This expression can be reduced to the standard heterogeneous bimorph deflection equation by considering a device with only two layers: one elastic and one piezoelectric, yielding the result given by (13). The subscripts  $e$  and  $p$  in

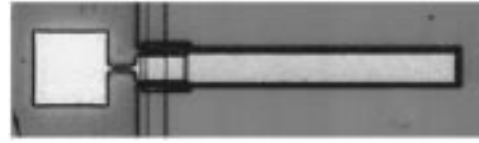


Fig. 3. Optical photograph of a ZnO multimorph.

TABLE I  
MULTIMORPH FILM PROPERTIES

Layer	thickness [ $\mu\text{m}$ ]	width [ $\mu\text{m}$ ]	E [GPa]	$\nu$
polysilicon	1.7	30	162	.23
$\text{Si}_x\text{N}_y$	0.2	26	290	.28
ZnO	0.5 / 1.0 / 1.5	26	161	.36
Pt	0.2	26	250	.25

this equation refer to the elastic and piezoelectric layers, respectively

$$\delta(x) = \frac{x^2 d_{31} \mathbf{E}_p (t_e + t_p) A_e E_e A_p E_p}{(t_e + t_p)^2 A_e E_e A_p E_p + 4(A_e E_e + A_p E_p)(E_e I_e + E_p I_p)}. \quad (13)$$

Assuming the elastic and piezoelectric layers have the same width and with the applied electric field given by  $\mathbf{E}_p = V/t_p$ , where  $V$  is the applied voltage, (13) can be further reduced to (14). This expression is precisely equivalent to the predicted deflection given by Smits for a piezoelectric heterogeneous bimorph [3]

$$\delta(x) = \frac{3t_e(t_e + t_p)E_e E_p x^2 d_{31} V}{E_e^2 t_e^4 + E_e E_p (4t_e^3 t_p + 6t_e^2 t_p^2 + 4t_e t_p^3) + E_p^2 t_p^4}. \quad (14)$$

### III. TEST STRUCTURE FABRICATION

A number of four-layer multimorphs were constructed using surface micromachining techniques to allow comparison of

$$\begin{bmatrix} \frac{1}{A_1 E_1} & \frac{-1}{A_2 E_2} & 0 & \cdots & 0 \\ 0 & \frac{1}{A_2 E_2} & \frac{-1}{A_3 E_3} & 0 & \cdots \\ \cdots & 0 & 0 & \cdots & \cdots \\ 0 & \cdots & 0 & \frac{1}{A_{m-1} E_{m-1}} & \frac{-1}{A_m E_m} \\ 1 & 1 & \cdots & 1 & 1 \end{bmatrix} \cdot \begin{bmatrix} F_1 \\ F_2 \\ \cdots \\ F_{m-1} \\ F_m \end{bmatrix} - \frac{1}{2r} \begin{bmatrix} t_1 + t_2 \\ t_2 + t_3 \\ \cdots \\ t_{m-1} + t_m \\ 0 \end{bmatrix} - d_{31} \begin{bmatrix} \mathbf{E}_2 - \mathbf{E}_1 \\ \mathbf{E}_3 - \mathbf{E}_2 \\ \cdots \\ \mathbf{E}_m - \mathbf{E}_{m-1} \\ 0 \end{bmatrix} = \begin{bmatrix} 0 \\ 0 \\ 0 \\ 0 \\ 0 \end{bmatrix}$$

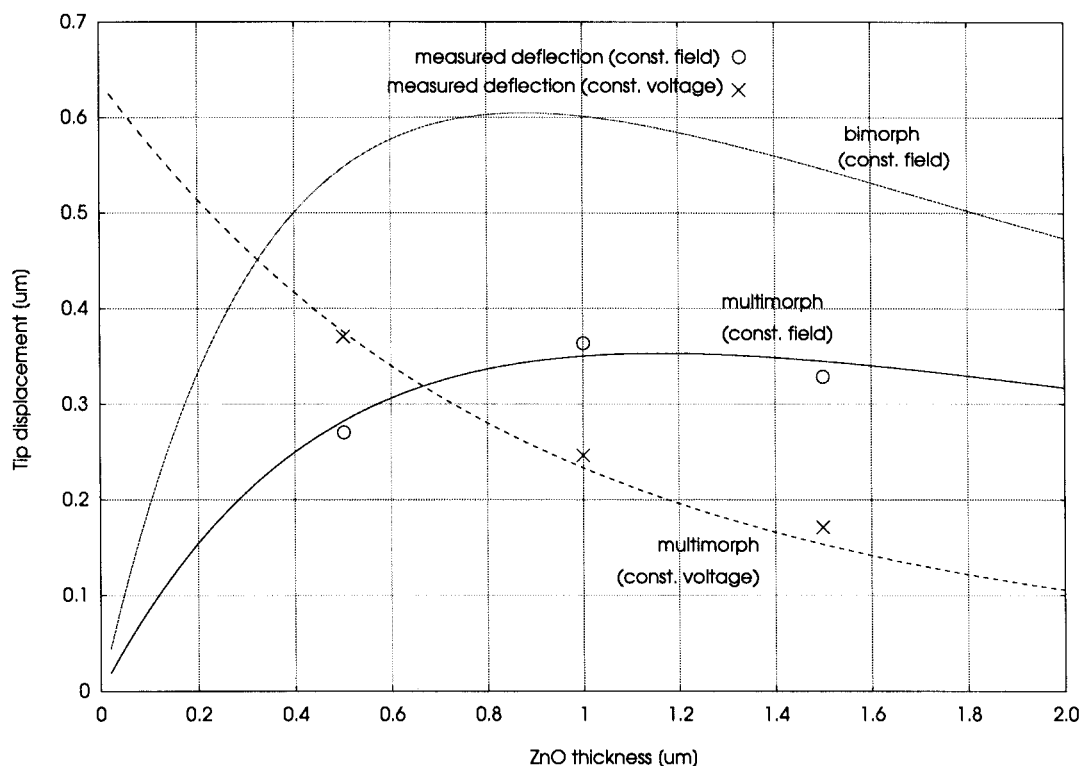


Fig. 4. Experimental versus theoretical deflection at constant voltage (2 V) and constant field (3 V/ $\mu\text{m}$ ). The third curve reflects the deflection predicted by the standard bimorph assumption at constant field (3 V/ $\mu\text{m}$ ).

the deflection model given by (12) with experimental results. The multimorph structure, shown in Fig. 2, consists of a base layer of polysilicon, which acts as the primary elastic layer and bottom electrode for the piezoelectric layer, a  $\text{Si}_x\text{N}_y$  layer, which provides an amorphous seed layer for the ZnO [6] and allows low-frequency actuation of the device [7], a ZnO piezoelectric layer, and finally a Pt top electrode. ZnO was chosen as the piezoelectric material for this study due to its relatively high-transverse-coupling coefficient ( $d_{31}$ ) and well-understood fabrication techniques.

The multimorph test structures were fabricated as follows. Starting with a  $\langle 100 \rangle$  silicon wafer with a thin silicon nitride passivation layer, a ground layer of low-pressure chemical-vapor deposition (LPCVD) phosphorus-doped polysilicon was deposited and patterned via reactive ion etching (RIE). This layer serves as a bottom electrode contact. A  $2.0\text{-}\mu\text{m}$  layer of oxide was then deposited and patterned via plasma etching to define the vertical offset of the multimorph beams. Next, a  $1.7\text{-}\mu\text{m}$  layer of phosphorus-doped polysilicon was deposited and etched in a  $\text{Cl}_2$  plasma, defining the primary elastic element of the multimorph structure. The polysilicon is highly doped to provide a low-resistivity lower electrode for the piezoelectric material. A thin  $0.2\text{-}\mu\text{m}$  layer of LPCVD silicon nitride was then deposited followed by a layer of RF-magnetron-sputtered ZnO from an undoped target and  $0.2\text{ }\mu\text{m}$  of sputtered Pt. The ZnO was deposited with three different thicknesses of  $0.5$ ,  $1.0$ , and  $1.5\text{ }\mu\text{m}$ . A rapid thermal annealing step was then performed for 5 min at  $500\text{ }^\circ\text{C}$  in order to reduce the highly compressive residual stress of the ZnO. The  $\text{Si}_x\text{N}_y$ , ZnO, and Pt layers were patterned in a single etch by masking

selected structures with  $4\text{ }\mu\text{m}$  of photoresist and ion-milling each layer in a single etch. This approach to etching was found to provide excellent control of device geometry compared to both wet etching and RIE. The structures were then released using a photoresist mask in 5:1 buffered hydrofluoric acid (BHF) followed by a supercritical  $\text{CO}_2$  drying step to avoid sticking of the beams to the substrate. Finally, the photoresist masking layer was removed by  $\text{O}_2$  plasma ashing. An optical photograph of a multimorph fabricated using this process is shown in Fig. 3.

#### IV. EXPERIMENTAL RESULTS

In order to compare the theoretical deflection model of a multimorph with experimental results, three  $500\text{-}\mu\text{m}$ -long multimorphs with varying ZnO thicknesses were actuated by applying a dc voltage between the upper and lower electrodes and measuring the deflection at the tip. The experiments were carried out under two distinct conditions. In the first case, the applied voltage was held fixed for each of the devices (constant voltage, 2 V), while in the second case, the voltage was scaled proportional to the thickness of the piezoelectric layer (constant electric field, 3 V/ $\mu\text{m}$ ). The constant voltage condition corresponds to the case, where the maximum driving voltage is externally constrained, for example, when the drive electronics provide a limited output swing due to the use of low-voltage circuits. The constant field condition is relevant when the maximum field is limited by the breakdown field of the piezoelectric film. Both cases are important to consider for predicting the maximum deflection achievable under each of these operating regimes.

Deflections were measured under both electrical boundary conditions for each of the three multimorphs. Atomic force microscopy (AFM) was used to perform deflection measurements as this technique allows for precise positioning of the point of measurement, ensuring that measurements were taken as near to the beam tip as possible.

The multimorph parameters are given in Table I. The absolute value of the resulting theoretical and experimental deflections are plotted against ZnO film thickness as shown in Fig. 4. In this figure, the solid and dashed curves are the modeled deflection curves for constant field and constant voltage, respectively. The third curve indicates the deflection, which results from application of the bimorph assumption, given by (13), at constant field, i.e., omission of the nitride and platinum layers from the analysis. As shown in the figure, the multimorph model provides a relatively good fit to the experimental data, while the bimorph assumption results in significant error, thus demonstrating the utility of the multimorph model.

The value of  $d_{31}$  used in generating the modeled curves in Fig. 4 was not known *a priori*. In fact, given a multimorph with well-known geometry and mechanical properties for each layer, the multimorph model provides a method for measuring  $d_{31}$  by finding the value, which minimizes the error between predicted and experimental deflection data. Using this approach, a value of  $d_{31} = -2.3$  pC/N was determined for the transverse-coupling coefficient of the ZnO used for the experimental test structures. Note that in generating the theoretical curves, the same value of  $d_{31}$  was employed for both the multimorph and bimorph models. If  $d_{31}$  had been measured by fitting the data to the bimorph curve, the resulting value would have been nearly  $2x$  smaller in magnitude than the above value of  $-2.3$  pC/N.

One interesting result evident from Fig. 4 can be seen by comparing the constant field curves for the bimorph and multimorph models. For the bimorph case, maximum deflection is predicted for a ZnO thickness of approximately  $0.9 \mu\text{m}$ , while for the multimorph case, this value is  $1.2 \mu\text{m}$ : in order to achieve maximum deflection under constant field for a multimorph device, the optimal ZnO thickness is about  $0.3 \mu\text{m}$  larger than what would be expected if the bimorph model had been used during the design process. This result does not apply for the constant voltage case since, here, the deflection always increases as the piezoelectric film thickness is reduced, regardless of which model is employed. Thus, when designing for a voltage-limited drive signal, the optimal thickness for the piezoelectric layer is given by the thinnest achievable film based on either breakdown field or fabrication constraints.

## V. CONCLUSIONS

A model has been derived, which describes the deflection of a generic  $m$ -layer piezoelectric multimorph. Experimental measurements from a series of  $500\text{-}\mu\text{m}$ -long cantilever devices agree well with the multimorph model, although this agreement depends on an assumed  $d_{31}$  value. The derived model was shown to be significantly more accurate than the standard

bimorph model. For the case of a constant applied voltage, it was shown that the optimal piezoelectric film thickness is always given by the thinnest achievable film, while for a constant applied field, the multimorph model should be employed to determine the optimal thickness.

## ACKNOWLEDGMENT

The authors would like to thank J. Bustillo (Berkeley Sensor and Actuator Center) for his input on device fabrication and A. Lal (BSAC) and R. Hsiao (Department of Mechanical Engineering, University of California at Berkeley) for their assistance with nanoindentation experiments for ZnO elastic modulus measurements.

## REFERENCES

- [1] S. Timoshenko, "Analysis of bi-metal thermostats," *J. Optic. Soc. Am. Rev. Sci. Inst.*, vol. 11, no. 3, pp. 233-56, 1925.
- [2] W.-H. Chu, M. Mehregany, and R. L. Mullen, "Analysis of tip deflection and force of a bimetallic cantilever microactuator," *J. Micromech. Microeng.*, vol. 3, no. 1, pp. 4-7, 1993.
- [3] J. G. Smits and W.-S. Choi, "The constituent equations of piezoelectric heterogeneous bimorphs," *IEEE Trans. Ultrason., Ferroelect., Freq. Contr.*, vol. 38, no. 3, pp. 256-270, 1991.
- [4] J. G. Smits and A. Ballato, "Dynamic admittance matrix of piezoelectric cantilever bimorphs," *IEEE J. Microelectromech. Syst.*, vol. 3, no. 3, pp. 105-111, 1994.
- [5] *IEEE Standard on Piezoelectricity*, ANSI/IEEE Standard 176-1987.
- [6] S. Akamine, T. R. Albrecht, M. J. Zdeblick, and C. F. Quate, "A planar process for microfabrication of a scanning tunneling microscope," *Sens. Actuators*, vol. A23, no. 3, pp. 964-70, 1990.
- [7] F. R. Blom *et al.*, "Thin-film ZnO as micromechanical actuator at low frequencies," *Sens. Actuators*, vol. A21, no. 1, pp. 226-228, 1990.



**Don L. DeVoe** received the B.S. degree in mechanical engineering in 1991 and the M.S. degree in 1993, both from the University of Maryland at College Park (UMCP), and the Ph.D. degree in mechanical engineering from the University of California, Berkeley, in 1997.

He is currently an Assistant Professor in the Department of Mechanical Engineering, UMCP. His research interests include the integration of piezoelectric thin films for sensing and actuation of MEMS devices, with particular focus on inertial sensor applications.



**Albert P. Pisano** received the Ph.D. degree from Columbia University, New York, NY, in 1981, in the area of high-speed cam systems.

He joined the University of California, Berkeley, in 1983 after two and a half years as a Member of the Research Staff in the Mechanical Engineering Sciences area of the Xerox Palo Alto Research Center. He is currently an Associate Professor in the Department of Mechanical Engineering. He also held research positions at the General Motors Research Laboratory and the Singer Sewing Machine Corporate R&D Laboratory. In addition, he served as a Mechanical Design Consultant to Xerox, General Motors, TRW, Sunstrand, American Machinery, and Singer. He is active in the area of microelectromechanical systems and serves as a Director of the Berkeley Sensor and Actuator Center.

Dr. Pisano received the NSF Presidential Young Investigator Award in 1985 for research in optimal system design.